REPORT DOCUMENTATION PAGE

Form Approved
OMB NO. 0704-0188

1. AGENCY USE ONLY (Leave Blank)	2. REPORT DATE	3. REPORT TYPE AND DATES COVERED
	9 Feb 2008	Final 22 Jul 08 - 18 Jan 09

4. TITLE AND SUBTITLE
STTR Phase I: Electrostatic Atomizing Fuel Injector for Small Scale Engines

5. FUNDING NUMBERS
W911NF-08-C-0107

6. AUTHOR(S)
Farzad Mashayek

7. PERFORMING ORGANIZATION NAME(S) AND ADDRESS(ES)
Enabling Energy Systems Inc
9800 Connecticut Dr, Crown Point, IN 46307

8. PERFORMING ORGANIZATION REPORT NUMBER
EES-DD0010

9. SPONSORING / MONITORING AGENCY NAME(S) AND ADDRESS(ES)
U. S. Army Research Office
P.O. Box 12211
Research Triangle Park, NC 27709-2211

10. SPONSORING / MONITORING AGENCY REPORT NUMBER

11. SUPPLEMENTARY NOTES
The views, opinions and/or findings contained in this report are those of the author(s) and should not be construed as an official Department of the Army position, policy or decision, unless so designated by other documentation.

12 a. DISTRIBUTION / AVAILABILITY STATEMENT
Approved for public release; distribution unlimited.

12 b. DISTRIBUTION CODE

13. ABSTRACT (Maximum 200 words)

"Report developed under STTR contract W911NF-08-C-0107" for topic "A08-T012". The overall objective of this STTR project is to develop electrostatic atomizers for spraying JP-8 fuel in small scale internal combustion engines. This report discusses the efforts of Phase I where it has been demonstrated that the proposed charge injection method can be used for atomization of JP-8. The characteristics of sprays formed with JP-8 are found to be very similar to those of sprays formed with diesel fuel using the same method of atomization, regardless of a difference in electrical conductivity coefficients of these fuels. This important finding allows us to use the extensive previous knowledge on diesel fuel to understand the atomization of JP-8. The above demonstration of JP-8 atomization was based on an existing point-blade charge injector. Further investigation has been conducted in Phase I to improve this design in order to achieve higher specific charges and higher fuel flow rates. One design of the new atomizer was successfully tested and the data presented in this report support the improvement of the spray characteristics. Finally, new concepts have been investigated to apply the method of charge injection in conjunction with a pulse fuel delivery system which is required for internal combustion engines.

14. SUBJECT TERMS
STTR report, Electrostatic atomization, small engine, fuel injector, electrically-insulating fuel, IC engine

15. NUMBER OF PAGES
36

16. PRICE CODE

17. SECURITY CLASSIFICATION OR REPORT	18. SECURITY CLASSIFICATION ON THIS PAGE	19. SECURITY CLASSIFICATION OF ABSTRACT	20. LIMITATION OF ABSTRACT
UNCLASSIFIED	**UNCLASSIFIED**	**UNCLASSIFIED**	**UL**

NSN 7540-01-280-5500

Standard Form 298 (Rev.2-89)
Prescribed by ANSI Std. 239-18
298-102

Enclosure 1

Foreword

This final technical report summarizes our accomplishments in Phase I. As the report indicates, not only all the proposed goals in Phase I have been met, but also several new initiatives were taken as deemed necessary for Phase II planning.

In Phase I, it has been demonstrated that the proposed charge injection method can be used for atomization of JP-8. The characteristics of sprays formed with JP-8 were found to be very similar to those of sprays formed with diesel fuel using the same method of atomization, regardless of a difference in electrical conductivity coefficients of these fuels. This important finding allows us to use the extensive previous knowledge on diesel fuel to understand the atomization of JP-8. The above demonstration of JP-8 atomization was based on an existing point-blade charge injector. Further investigation has been conducted in Phase I to improve this design in order to achieve higher specific charges and higher fuel flow rates. A multi-orifice design of the atomizer was successfully tested and the data presented in this report support the improvement of the spray characteristics. Finally, new concepts have been investigated to apply the method of charge injection in conjunction with a pulse fuel delivery system which is required for internal combustion engines.

The main body of the report is divided into four parts. Parts I and II discuss the practical and theoretical aspects of the work, respectively. Part III describes our initiatives taken after visiting VTD in Cleveland in the beginning of Phase I. As a result of this visit, the exact small engine used by VTD has been installed in our laboratory and is connected to the same dynamometer as that used at VTD. In addition, we have set up a test rig to separately study a standard pulse injection system. Finally, Part IV provides a summary of our capabilities as we prepare for Phase II.

Table of Contents

List of figures

List of tables

Statement of the problem studied

The information in this section is extracted directly from the Phase I proposal to describe the objectives of the work and the plan to meet them. As the following sections, divided into four parts, indicate, all of the proposed tasks were successfully conducted and, in addition, several other important initiatives were taken as they deemed necessary for the planning of Phase II.

Objective

The objective of the research proposed is to develop electrostatic fuel injectors for small direct injection internal combustion engines.

To achieve this objective the following scientific issues need to be addressed:

- A more complete understanding of the dominance of several competing fluid and electrical timescales, with respect to timescales associated with a pulsed fuel injection event.
- Further timescale limitations associated with small length and timescales associated with creating combustible mixtures in small direct injection internal combustion engines with jet fuel blends, such as JP-8.

In additions, solutions to the following technological issue need to be defined:

- Developing an electrostatic fuel injection system of low weight, low power consumption, and robustness to be used in a military context.

Approach

The overall STTR project aims by phase are as follows:

- PHASE I: Design, develop and demonstrate an electrostatic atomizer that will enable atomization of JP-8 fuel (as specified by MIL-DTL-83133E, 1999) sufficient to be used in a small scale (5 hp) spark ignition engine. Deliver a plan for achieving pulsed atomization to enable Direct Injection Spark Ignition (DISI) in Phase II.
- PHASE II: Design, develop and demonstrate a pulsed injection electrostatic atomizer which enables a 5 hp flight-weight engine in a DISI cycle using JP-8 fuel (as specified by MIL-DTL-83133E). Deliver one system to the Army.
- PHASE III Dual Use: Development of electrostatic atomization injectors to enable DISI cycle on small scale engines with low-volatility fuels (JP-8 and DF-2) will allow higher efficiency, improved emissions and increased safety for small scale engines in widespread use throughout the commercial community.

The Phase I program is focused on:

- Demonstrating spray combustion proof of concept of JP-8 using a low pressure (~1 bar gauge) atomization system.
- Scoping out various design requirements in terms of pulsed spray quality and system components, matched to the engine and fuel specification.
- Establishing computational methods that will underpin the development of the fuel injection system in Phase II.

Phase I Work Plan:

Task\month	Location	1	2	3	4	5	6
T1: Engine/spray timescale analysis	UIC	X	X				
T2: Injection mode analysis	UIC				X		
T3: JP-8 charged spray 2D CFD simulations	UIC	X	X	X	X	X	X
T4: Charge injection boundary condition verification in 1D	UIC			X	X		
T5: Preliminary 2D EHD simulation of atomizer internal flow	UIC					X	X
T6: JP-8 charge injection single-orifice atomizer evaluation	UIC	X					
T7: Multi-orifice atomizer development	EES		X	X	X	X	
T8: Multi-orifice atomizer electrical evaluation with JP-8	UIC				X		X
T9: Multi-orifice atomizer spray evaluation with JP-8	UIC					X	
T10: Multi-orifice atomizer combustion evaluation with JP-8	UIC						X
T11: Fuel system selection/design	EES	X	X	X	X	X	X
T12: Pulsed HV system design	EES			X	X	X	X
T13: Phase II work plan definition	EES						X
T14: Collaboration with the ARL's Vehicle Technology Directorate	EES					X	X
T15: Progress report	EES	X	X	X	X	X	X
T16: Progress meetings with PO	EES			X			X

Milestones:

Milestone 1: "Demonstrate that JP-8 can be successfully electrostatically atomized and dispersed using the charge injection technique"

JP-8 has specific requirements in terms of its physical properties, including electrical conductivity (MIL-DTL-83133E, 1999), therefore, there is a need to confirm that the charge injection method is viable for this fuel (T6).

Milestone 2: "Develop the atomizer design such that a spray of JP-8 fuel sufficient to be used in a small lightweight spark ignition engine is produced."

There are three aspects to this milestone:

1. Define the required spray characteristics in terms of mean drop diameter (Task T1).
2. Define the spray characteristics in terms of mean spray charge required (Task T3).
3. Design charge injection technology that will produce sufficiently small drops of JP-8 at sufficiently low fuel supply pressure (Tasks T7 to T10).

Milestone 3: "Deliver a plan for achieving pulsed atomization to enable Direct Injection Spark Ignition in Phase II."

There are 5 aspects to this milestone:

1. Understanding the transient injection regime within the atomizer (Task T1)
2. Development of a charge injection model for CFD code implementation (Task T4)
3. Preliminary results from CFD prediction of the atomizer internal flow (Task T5)
4. Fuel system selection/design (Task T11)
5. Pulsed high-voltage (HV) system design (Task T12)

PART I: Design, manufacturing, and testing

I.1 JP-8 charge injection single-orifice atomizer evaluation

The first and most crucial task was to demonstrate that JP-8 can be successfully sprayed with our electrostatic atomization method, without using any additives to alter the conductivity of the fuel. Samples of standard JP-8 were obtained from Dr. Tim Edwards at AFRL. These samples were tested in our existing point-plane electrostatic atomizer (discussed in the Phase I proposal), and the results were compared with the existing diesel oil data-set obtained during the last year. Figure 1 shows the total current injected into the fuel and the portion of it carried away by the fuel as the spray current. A higher spray current leads to a higher spray specific charge hence more efficient atomization of the fuel.

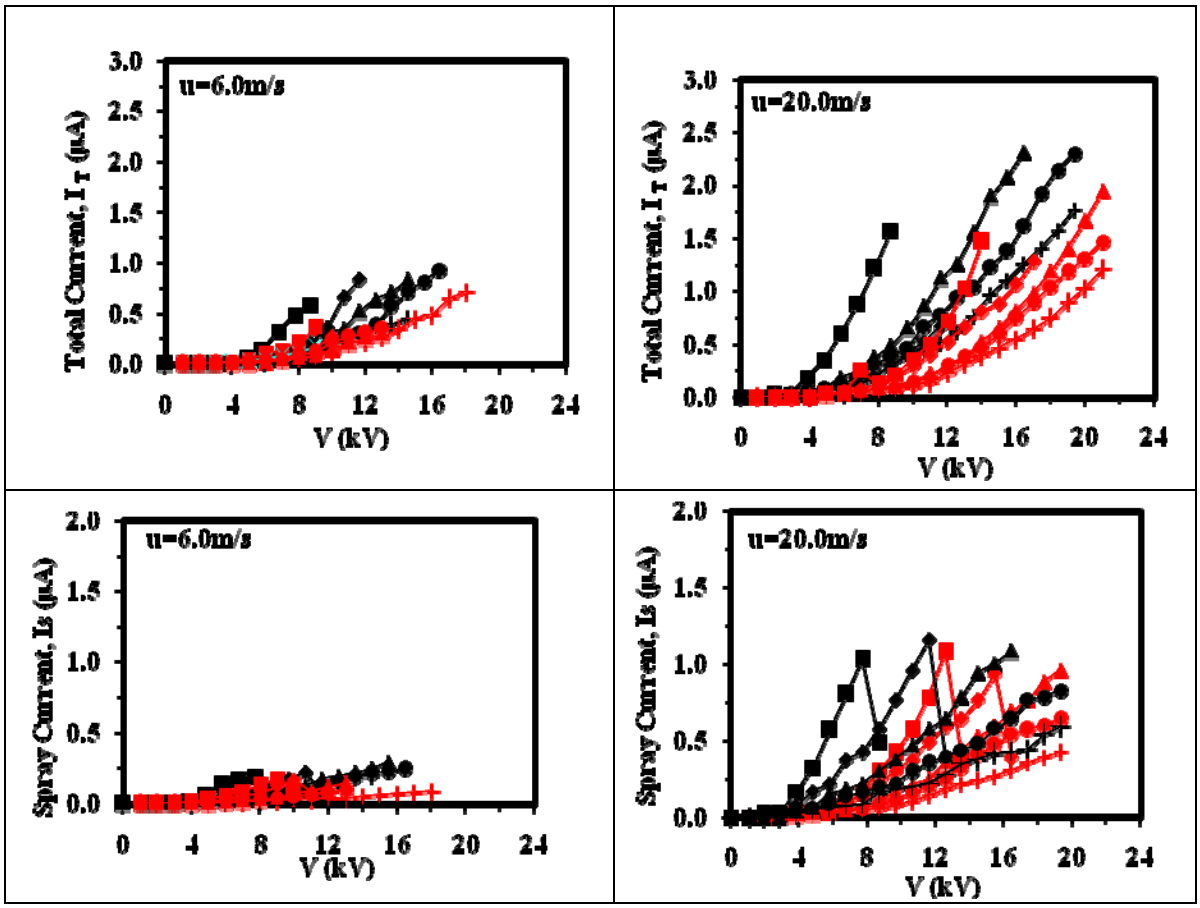

Figure 1: Total (top row) and spray (bottom row) currents for diesel oil (red) and JP-8 (black) at two different injection velocities.

Figure 1 is an important result because there are very specific restrictions on the electrical conductivity of JP-8, whereas there are none for standard US diesel as far as we are aware. The result shows that JP-8 is typical of other tested hydrocarbon liquids studied over the last decade and that the knowledge gained during this previous work can be applied to JP-8.

I.2 Multi-orifice charge injector

To improve upon the point-plane design, in Phase I a new multi-orifice charge injector was designed, constructed, and tested. The multi-orifice injector is more efficient in that

- It allows larger flow rates which are needed for combustion applications.
- It eliminates the sensitivity to the alignment of the needle and the orifice which was an issue for the point-plane design.
- It achieves higher specific charges, leading to smaller droplet sizes thus better combustion.

Therefore, the point-plane injection concept, where the small radius high voltage point (typically a needle tip) is placed above the orifice inside the atomizer, was modified. A blunt electrode and an array of orifices placed underneath it were used in the new design. The details of the multi-orifice design are given in Appendix A. Below, some of the results from the experiments are presented.

Figures 2 and 3 show the spray current (I_S) and the total current (I_T) vs. the applied voltage (V), respectively, for single 125 μm orifice diameter compared with 3 same size orifices their centers located at 1 mm equal sides lengths triangle corners. These results are shown for diesel fuel at fixed average jet velocity of 10 m/s and electrode distance from orifice inlet (L) to orifice diameter (d), L/d ratio, of 0.6, 1.0 and 2.0 using same sharp flat edge 3.2 mm diameter Tungsten electrode. As seen from Fig. 2, for $L/d \leq 1.0$, the maximum I_S which could be achieved with 3 orifices is approximately three times higher than that with the single orifice. Thus, I_S scaled approximately 1 to 1 ratio with increasing the number of orifices while maintaining the average jet velocity constant. This allowed maintaining maximum specific charge constant while increasing the number of orifices and atomizer flow rate, thus making the atomizer more useful in higher flow rate applications. Increasing specific charge enhances spray by producing smaller droplets sizes and increasing their dispersal rates.

The increase in I_S with increasing the number of orifices and flow rate for the same average jet velocity seems to be mainly related to the forced convection of emitted charge from electrode by the liquid velocity between electrode and orifice disk. The electric field and thus the charge emitting from the bottom of the flat electrode is distributed uniformly. Since the flow is axi-symmetric between the electrode bottom flat surface and the orifice disk, this allowed flow stream to each orifice to carry the same amount of emitted electric charge contributing to have the same spray charge for each orifice. In addition to the easiness of positioning electrode from orifice inlet precisely with using a flat sharp edge electrode compared with the needle electrode, it allows distributing emitted charge uniformly to each individual orifice, thus making spray from the multi-orifices uniform having same droplets sizes and distribution. As seen from Fig. 2, atomizer optimal performance seems to occur at L/d between 0.6 and 1.0 where the maximum specific charge could be achieved and at reasonably low applied voltage values.

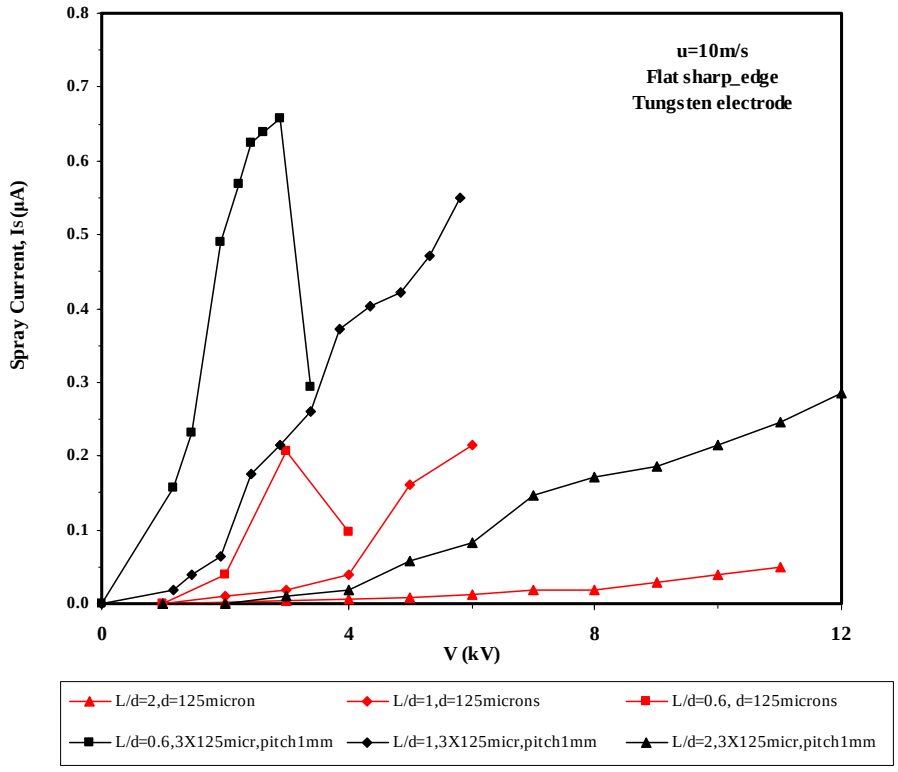

Figure 2: Spray current from 1x and 3x hole orifice systems.

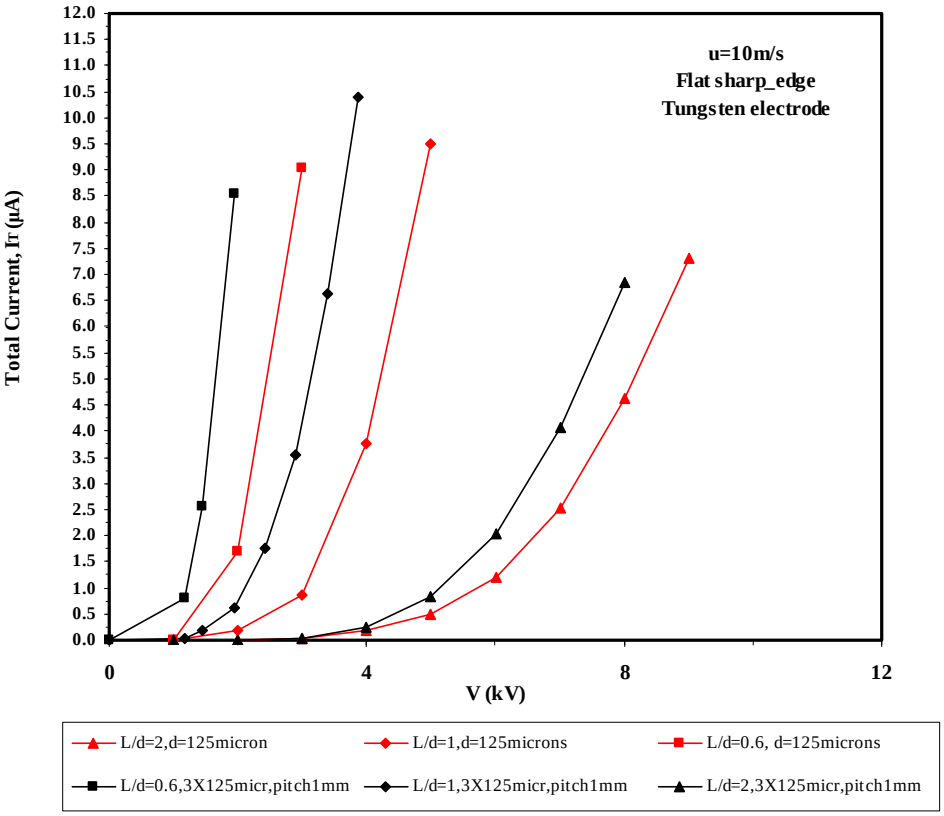

Figure 3: Total current from 1x and 3x hole orifice systems.

Whilst developing the multi-orifice atomizer concept, we wanted to ensure that the hole to hole variability of each jet and subsequent spray was small. This is most easily achieved using photography, and visually checking that the jet break up lengths and spray dispersal rates are similar between different jets. Figure 4 shows a single photograph from a 3 hole d=125 micron orifice plate, spraying diesel oil at 10 m/s per jet. As can be seen hole to hole variability is minimal, leading us to conclude that the multi-orifice atomizer concept is robust and viable.

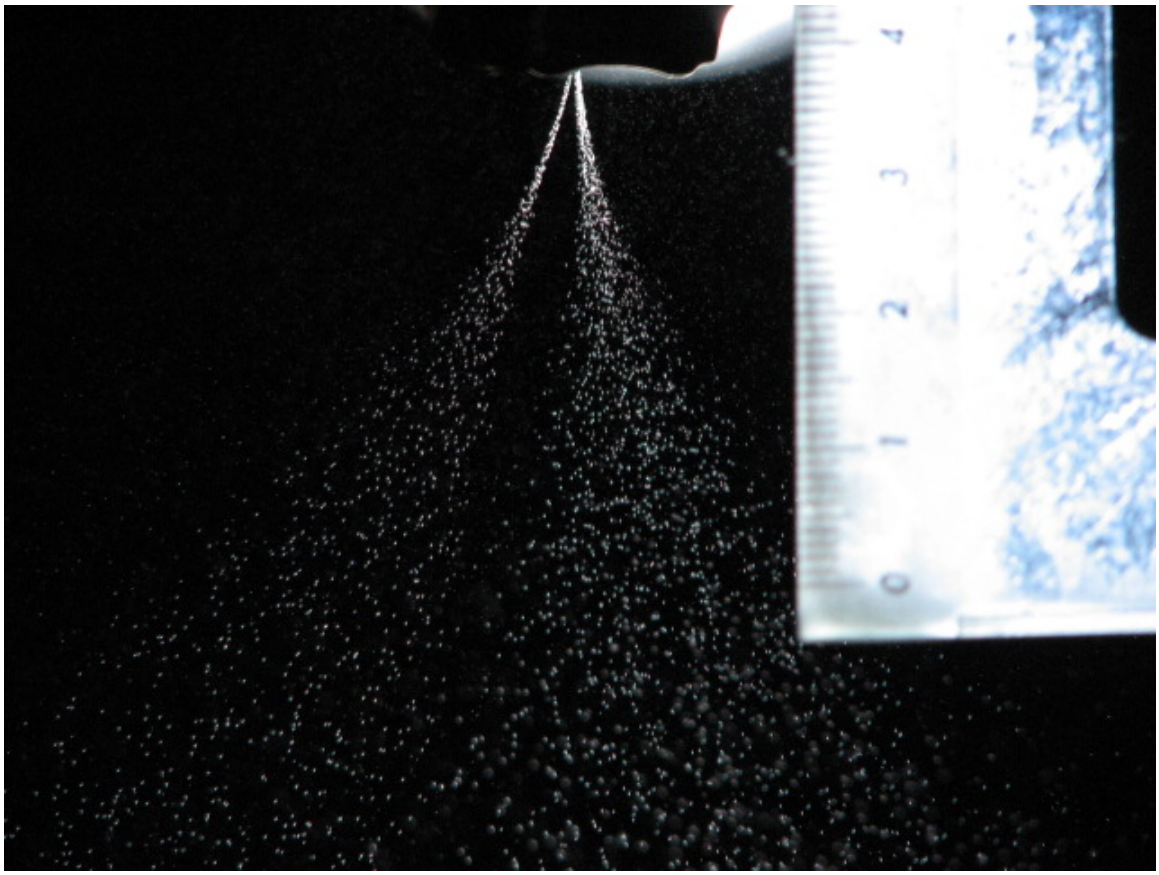

Figure 4: A multi-hole charge injection spray.

Figure 5 shows the spray specific charge (Q_S) vs. the applied voltage (V) for 3x80 µm, 0.50 mm pitch, orifices compared with 3x125 µm, 1.0 mm pitch, orifices for injected diesel fuel at velocity u = 10 m/s. Results are shown for L/d ratios of 0.6, 1.0 and 2.0. As seen from this figure, the maximum Q_S achieved with 3x80 µm orifices is about the same compared with the 3x125 orifices µm for low L/d ratios of 0.6 and 1.0. With the 80 µm orifices, the spray current and thus specific charge increase was limited by liquid electrical breakdown which was seen by arching (tripping) of the high voltage power supply. Such electrical breakdown is seen and documented by others for this method of atomization with such low flow rates (9 mL/min). The number of orifices is required to be increased in order to increase the flow rate and prevent such electrical breakdown and thus removing the limits from increasing the specific charges. For the higher L/d ratio of 2.0, the level of the specific charge is low and not useful in creating a full spray. Thus, the atomizer optimal electrical performance could be achieved with L/d < 1.0 for the 80 µm orifices.

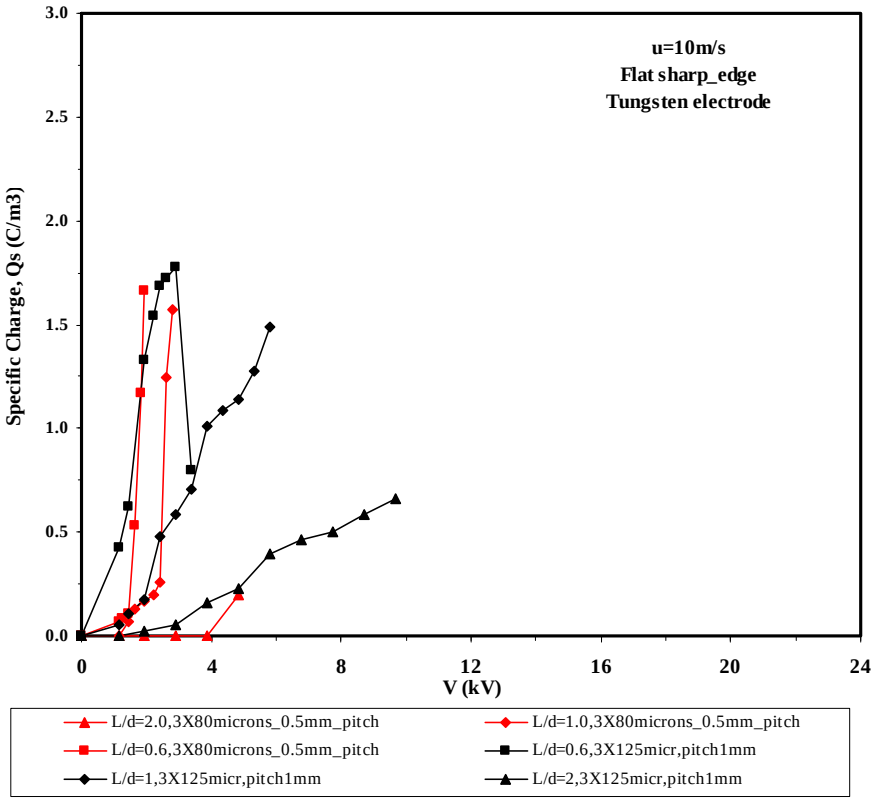

Figure 5: Spray specific charge for 80 micron orifice arrays.

The important conclusion from this study is that the blunt electrode/multi-hole design requires small gaps to work well (with a constraint of flow blocking due to too many orifice holes, which will be addressed in Phase II). These small gaps require much lower voltages than the point-plane design (i.e. 1-2 kV rather than 8-10 kV). This discovery makes the development of small cheap pulsed HV sources more viable.

Finally, a rig was set up to demonstrate the combustion of JP-8. As seen in Fig. 6, the laboratory is equipped with the necessary exhaust system for this purpose and has been previously used for similar combustion experiments. Unfortunately, we were not able to resolve all the safety issues during the limited time available to us in Phase I and, consequently, decided to postpone this experiment for Phase II. It must be mentioned that our group has already demonstrated the combustion of diesel fuel using the electrostatic atomization. Since the characteristics of sprays of JP-8 and diesel fuel are very similar, we do not foresee any particular difficulty with combustion of JP-8.

Figure 6: Combustion rig for JP-8.

I.3 Segregated blade-plane charge injector

In phase II, we intend to evaluate two EHD pulsed injector systems. The first is to develop an integrated atomizer, where the high-voltage electrode is an integral part of the pulsed fuel atomizer. The second is to separate the charge injection process from the atomization process. We intend to demonstrate charge injection component of the segregated approach, and we need to ensure that the magnitude of the injection current is at least an order of magnitude greater than that generated by the existing steady state integrated atomizer systems.

In order to charge the fluid with the maximum amount of charge and at the same time being able to attach any nozzle, a design of a linear charge injector was considered so that a two-dimensional charge injection system was formed using multiple blades, as shown in the exploded view in Fig. 7.

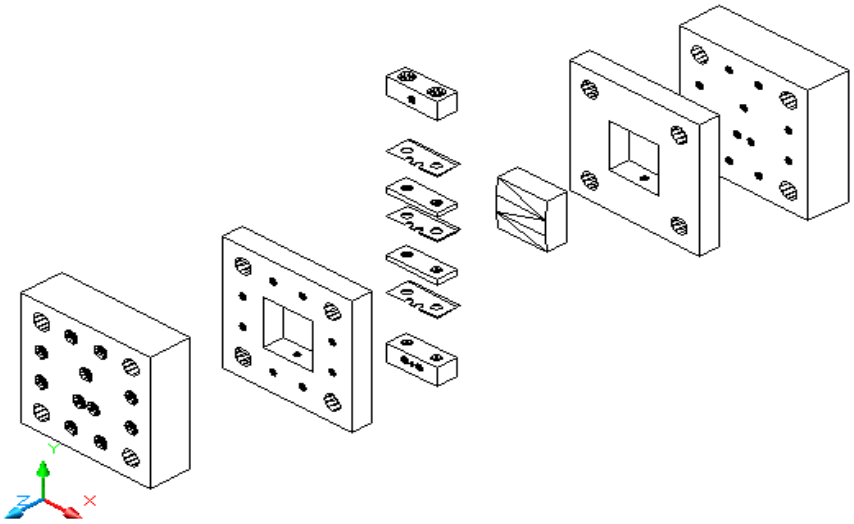

Figure 7: The high-current segregated charge injector. A series of razor blades are mounted in brass spacers and are connected to a high voltage supply. Current is emitted into the fluid, and some is conducted across it to a collector electrode (immediately right of the razor blade assembly). The entire system is housed within PTFE blocks.

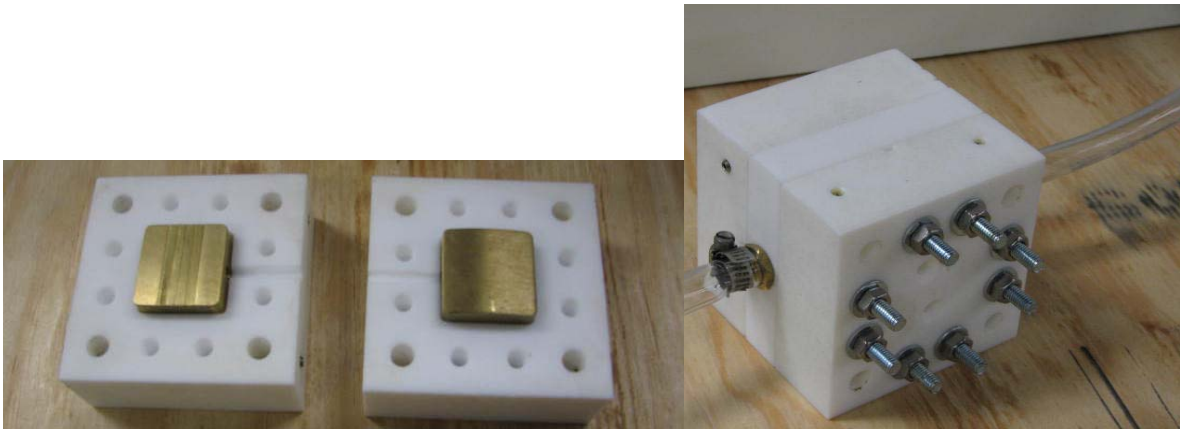

Figure 8: The blade-plane injector assembly.

The left image in Fig. 8 shows the high voltage blade assembly, the centre image shows the earthed collector electrode and the rightmost image shows the completed and assembled unit. It may be observed that a flow line is present in the assembled unit. This is to enable measurements under quiescent conditions and for forced flow conditions, to examine the viability of the technique.

First, experiments were conducted with the charge injection device in zero flow, using razor blades for our charge injection electrodes. A schematic of the rig is provided in Fig. 9, where the independent variables are the voltage, the blade gap and the curvature of the earthed collector electrode.

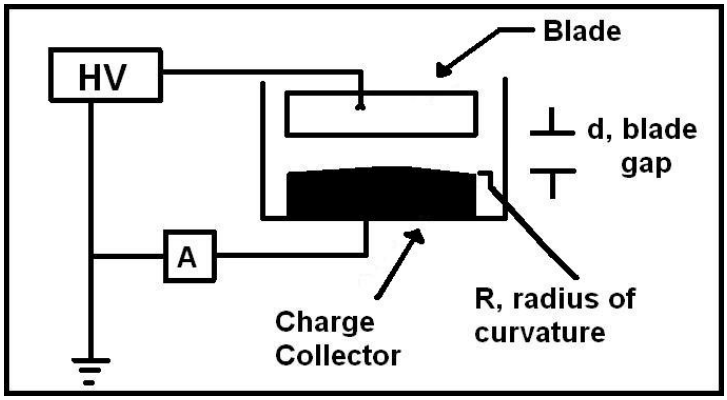

Figure 9: Schematic of the rig for no-flow experiments.

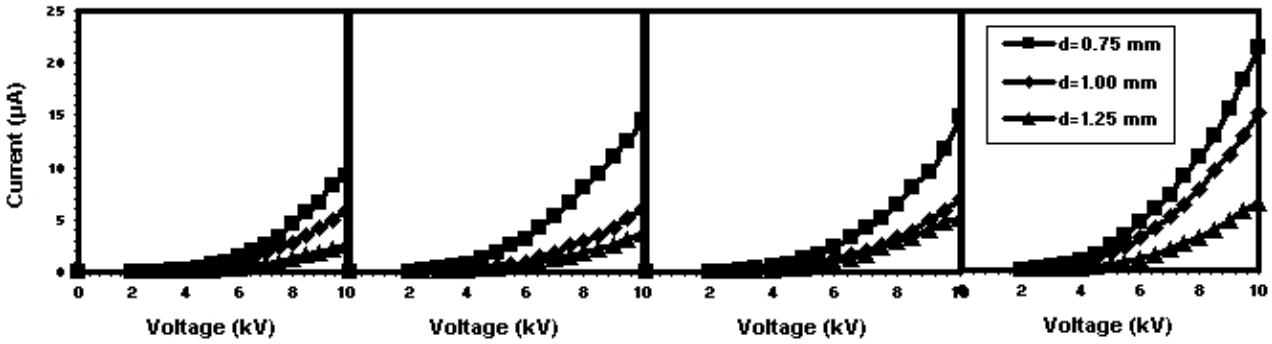

Figure 10: Comparison of the injected current in R= 75 mm, 100 mm, 125 mm and infinite (i.e. flat) rounded collector at three different gaps d=0.75 mm, 1.00 mm and 1.25 mm for diesel fuel with a single blade.

Figure 10 reports the results for a single blade, in terms of d and R (from left to right). A large curvature is more efficient, but was found to be more unstable, and it is advantageous to be able to modify the R parameter to optimize the requirements of power versus robustness. Figure 11 reports the results for multiple blades and here, although we do not find a perfect scaling of injected current increase, the improvement is significant.

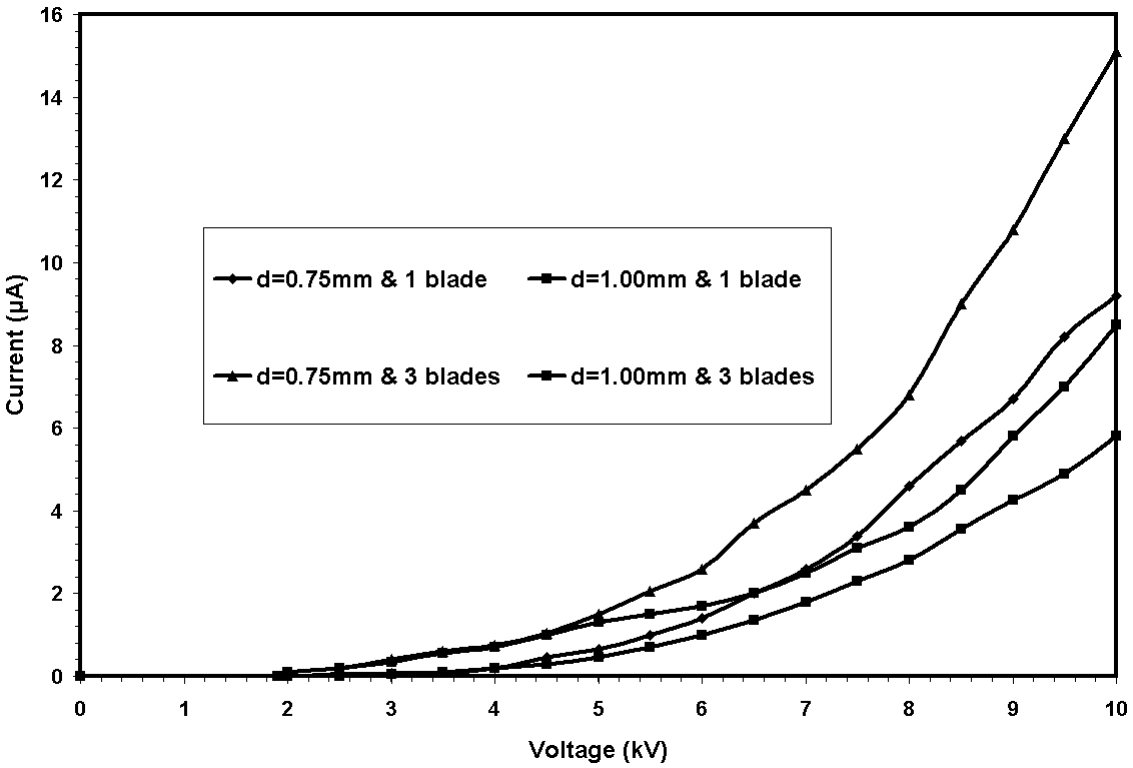

Figure 11: Single vs. multiple blades comparison for diesel fuel with 75 mm rounded collector.

After demonstrating that the blade injector works reliably for no-flow case, it was decided to build a new rig capable of high flow rates in the range of 0.1 to 0.5 l/s, as seen in Fig. 12. A 40–liter capacity stainless steel tank and a Sandpiper air-operated PTFE diaphragm pump were chosen for their compatibility with diesel fuel. A surge-protector was placed on top of the pump to ensure a steady flow.

An air exhaust line was built for the pump for more stable operations. Pumped fuel enters the fuel filter, which is capable of filtering particles bigger than 10 microns without a significant pressure drop. The volume of the clean fuel is measured by a digital flow-meter calibrated for diesel fuel. Then, fuel enters the charge injector. Two multi-meters are being used to measure leakage and spray currents.

Figure 12: The complete flow rig with blade charge injection system.

Finally, we conducted the high-flow charge injection experiments. Previously used injector was installed into a new rig capable of producing flow rates of 1-5 gpm with diesel fuel. Before running the experiments, computational studies were performed to have an idea of the flow pathlines and pressure drop inside the charge injector with one blade. Figure 13 shows large recirculation zones, increasing the fluid residence time.

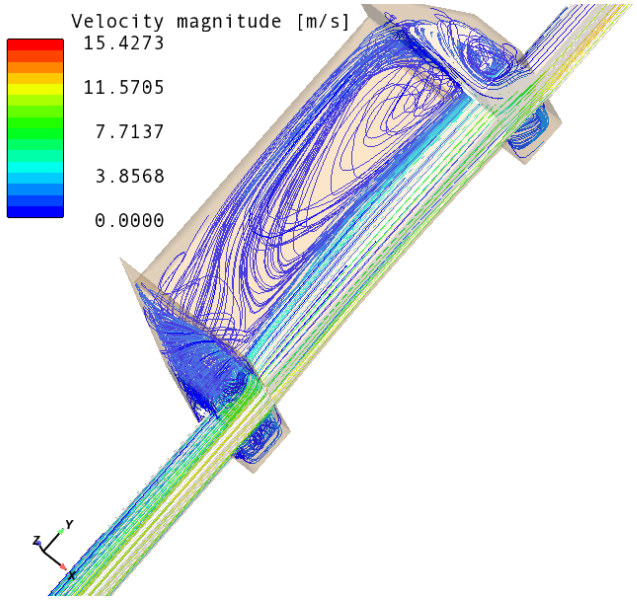

Figure 13: Predicted internal flow circulation within the blade system.

Figure 14 shows the effect of different blade gaps at constant flow rate on the liquid current (due to charges leaving the injector with the fuel) in the single-blade configuration. Closer gap between the blade and the electrode results in higher injected currents, as per the zero flow work.

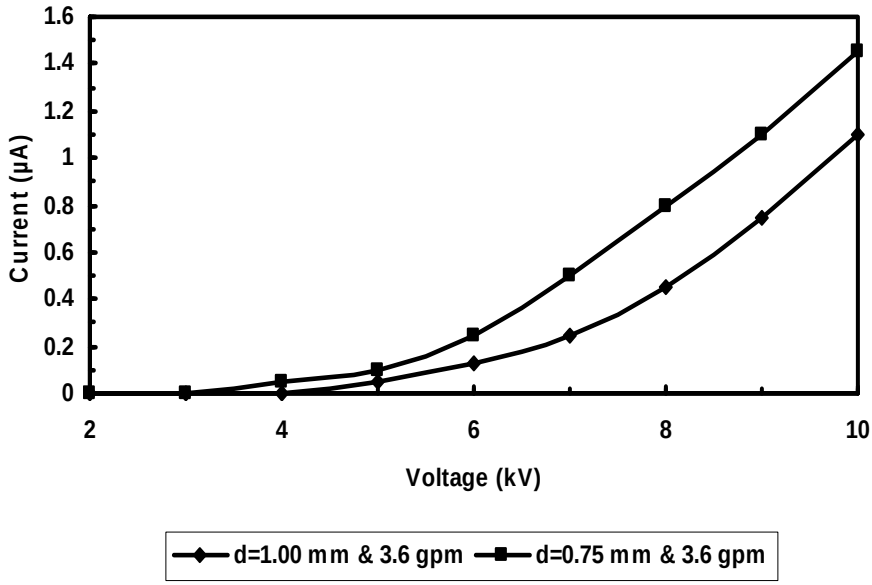

Figure 14: Injected current versus the blade gap at constant flow.

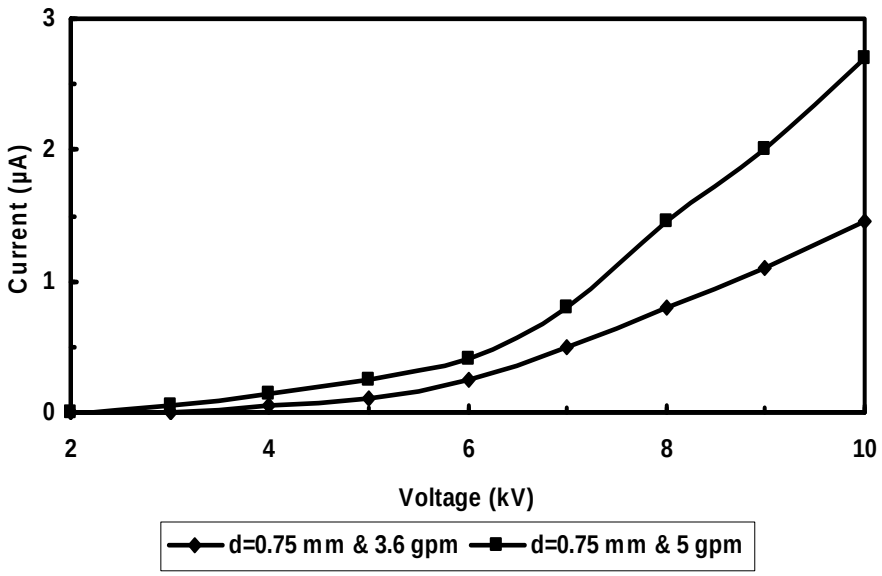

Figure 15: Injected current versus flow rate at constant blade gap.

Figure 15 confirms that we obtain an increase in the (injected) liquid current for higher flow rates, though the increase observed here is not significant. Design improvements are required to make this system practically useful. This will be tackled in Phase II.

I.4 Pulsed HV system design

We have conducted a survey of the available hardware in the commercial sector for high voltage equipment that can provide pulse trains with a high slew rate, summarized below.

Supplier	Model No.	Output Voltage	Rise Time	Pulse Width	avg. PRF	Power Supply	Dimensions (mm)	Weight (kg)	Delivery (months)	Cost
Moose-Hill	NPG-20	>20KV	<0.7ns	1-2ns decay	1 KHz	+5, +100, +0-300VDC	300x200x120		2	
Moose-Hill	PPG-20	>20KV	<100ps	1.5ns decay	1KHz	110/220V AC	300x230x120		2	
ITX-Harvar	ECM 830	3 kV		10 microsec		110 V/220 V	300x300x120	15	1	6826$
GBS	RUP6-25/3	25 kV	200 ns			230-240 V	00x550x1582		2	
GBS	ECOPULS 2	25 kV	5 μs	10-20 μs		230 V	83x267x600		2	
Mikrotek	PG 20 - 400	20 kV				230 V	55x604x80	100		
Microtek	IPG 2025	20 kV				230 V	50x180x51	18		

As can be seen typical weight, cost and size are not viable in terms of a small direct injection engine. Therefore, we will need to develop our own system for this purpose and this will need to be part of the Phase II development plan.

Given the complexity, and yet the importance, of this task, we have initiated a collaboration with Professor Sudip Mazumder from the Electrical and Computer Engineering at UIC. Professor Mazumder is

an expert in this area and will formally join our team in Phase II. In our preliminary discussions with Professor Mazumder, we have considered how to make use of small light but steady power high voltage supplies to construct a small light pulsed high voltage supply. We propose a modified circuit with an inductor and two switches that as switch 1 closes switch 2 will open (Fig. 16). The inductor will maintain a steady current. When 1 opens to stop a pulse, switch 2 will close to allow a path for the current in the inductor. Otherwise, with an open circuit, voltage in the inductor would spike.

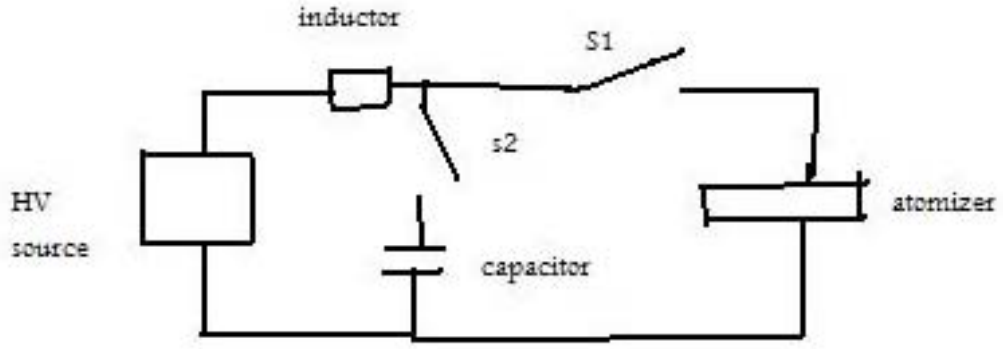

Figure 16: Preliminary sketch of high voltage switching circuit.

PART II: Computational/theoretical analysis

II.1 Timescale analysis

The objective of this study is to define the target drop diameter that the proposed electrostatic atomization system needs to generate to operate efficiently within a small direct injection spark ignition engine. Two factors are relevant here, the first are engine parameters, specifically geometry, speed and injection timing, the second is the use of JP-8, which has a longer heat up and evaporation timescale relative to the more usual liquid fuel, gasoline.

We have compared the global engine timescale (i.e. the time from fuel spray injection to ignition) against the representative timescale for drop deceleration, heat up and evaporation.

Figure 17 shows the global engine timescale as a function of engine speed for the two classical DISI injection strategies, injecting early (into the intake stroke, under full load) and injecting late (into the compression stroke, under part load). From Fig. 17, which applies to all engine sizes, it is clear that for late injection ($\theta_{inj} = 330^o$) the timescale constraint is severe regardless of engine speed, whereas for early injection ($\theta_{inj} = 230^o$) the timescale constraint is only relevant for higher engine speeds. Therefore, Fig. 17 gives us our baseline: drops should decelerate, heat up and evaporate within this global timescale.

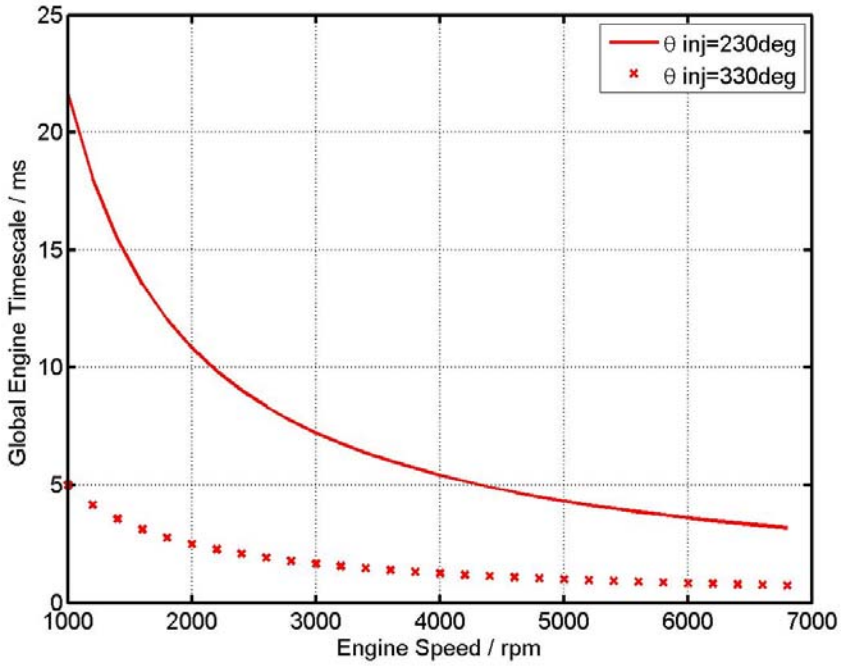

Figure 17: Global Engine Timescale (time between fuel injection and ignition) as a function of engine speed and an early and late injection strategy.

We have evaluated the drop deceleration, heat up and evaporation timescales against the global timescale shown in Fig. 17, and also a second engine timescale specific to drop deceleration, related to engine size, and piston position. Overall we find the most significant (i.e. limiting) drop timescale is that of mass transfer timescale and this is shown in Fig. 18.

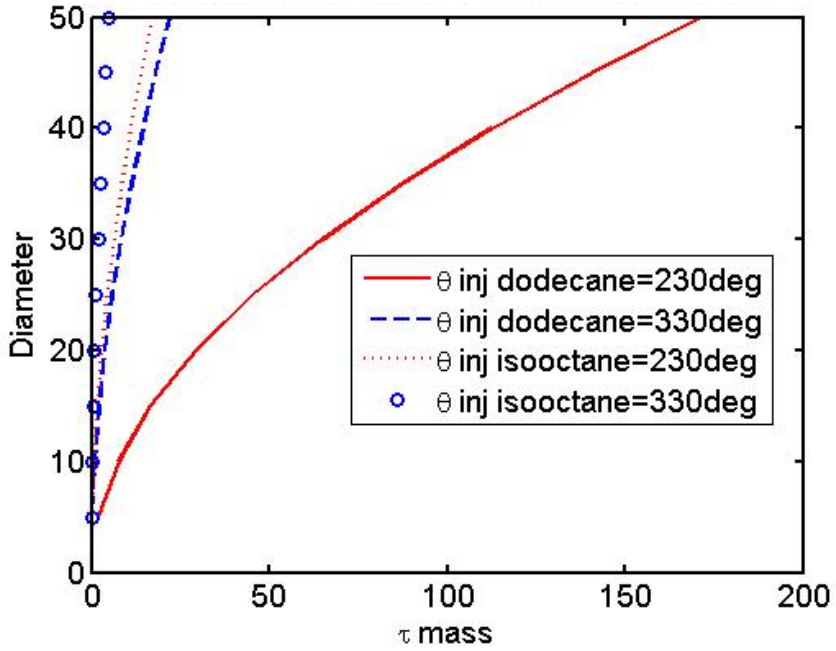

Figure 18: Droplet diameter (μm) vs. τ_{mass} (ms) for iso-octane and dodecane for two different injection strategies.

During the intake stroke, with an early injection strategy the fuel drop effectively sees air at normal temperature and pressure, whereas for late injection into the compression stroke the air has heated due to adiabatic compression. The result can be viewed as defining maximum permitted drop diameter for a given fuel and injection strategy at (with Fig. 17) a given engine speed. This figure shows the significant effect fuel properties *and* injection timing have upon the mass transfer timescale. Dodecane has been chosen as a surrogate for JP-8 since it is a major constituent of the surrogate fuel defined in [1]. We see values surpassing those of the global engine timescale values and now the restricting nature of the engine is made apparent.

The above analysis showed the relevant engine timescales, and how they are a strong function of the injection timing and the engine speed. It was also noted that amongst the drop timescales, that of mass transfer is the dominant timescale to consider. In other words, the evaporation timescale defines the maximum drop size the atomizer should generate and ensure the majority of the fuel mass has evaporated prior to ignition.

Effect of droplet secondary breakup

There is a limit to how much charge a droplet can hold before it breaks up and this is known as the Rayleigh limit,

$$Q_{ray} = \pi(\varepsilon_o \sigma)^{1/2}(2D)^{3/2} \tag{18}$$

where ε_o is the permittivity of the surrounding gas, σ is the surface tension of the fuel and D is the droplet diameter. As the droplet evaporates, the surface charge density increases until the Rayleigh limit is reached, leading to drop disruption. With some assumptions, as listed in Table 1, taken from the literature, we investigate this process in the acceleration of liquid evaporation.

Fuel Type	**Injection Regime**	**Charge Condition 1**	**Charge Condition 2**
Dodecane	Early injection@230CAD	$Q_{initial}=0.7Q_{ray}$ Break-up@ $Q=0.8Q_{ray}$ At each break up 80% of mass remains and 30% of charge remains. [1]	$Q_{initial}=0.4Q_{ray}$ Break-up@ $Q=0.8Q_{ray}$ At each break up 80% of mass remains and 30% of charge remains. [1]
	Late injection@330 CAD	Same as for early	Same as for early
Iso-octane	Early injection@230CAD	Same as above	Same as above
	Late injection@330 CAD	Same as above	Same as above

Table 1: Charge simulation parameters.

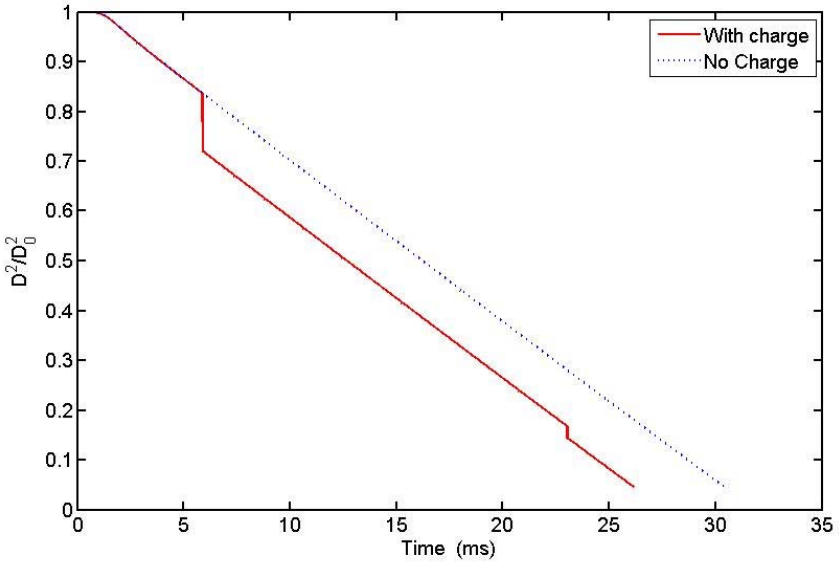

Figure 19: (D^2/D_o^2) vs. time for charge condition 1 of Table 1 for early injection.

As we can see from Fig. 19 charge has a significant effect on the evaporation of the droplet. The electric charge decreases the timescale taken for evaporation and can thus be used to enhance engine performance. Each discontinuity in the charged curve represents the droplet reaching the Rayleigh limit and thus losing 20% of its mass (to much smaller satellite droplets) and 70% of its charge.

II.2 Injection mode analysis

The injection mode analysis centres on examining the state of the fluid into which electric charge is injected by considering the relevant timescales and non-dimensional numbers. Relevant timescales are:

Viscous time: $\tau_\nu = L/\nu$

Ion drift time: $\tau_d = L/\kappa\phi$

Ion repulsion time: $\tau_C = \varepsilon/\kappa\rho_f$

where L is a characteristic length, ν the fluid viscosity, κ the ion mobility, ϕ the potential, ε the permittivity, and ρ_f the fluid density. The viscous time is the timescale associated with molecular diffusion, the ion drift time is the time taken for an ion to drift a distance *L* with a velocity κE. The ion repulsion time is the time taken for Coulomb repulsion to dissipate a given charge density ρ_f.

The ratio $C = \tau_d/\tau_C$ gives an injection strength parameter, and typically space charge limited injection occurs for C>10. Our scales in our charge injection atomizer suggest C >> 10, hence our injection is non-ohmic and space charge limited. Our experiments support this view.

We can also define a stability parameter, $T = \varepsilon\phi/\rho_f\nu\kappa$, which defines the ratio between the body force and viscous terms in the Navier-Stokes equations, in effect an electrical Rayleigh number. Our

scales in our charge injection atomizer suggest $T \sim O(5)$, leading us to conclude the fluid is highly chaotic.

Small engine spray simulation

The basis for the simulations is a set of results found in [2]. This outlined the dynamics of an electrically charged spray of iso-octane, generated by a typical (non-EHD) automotive pressure swirl atomizer, and included the effects of a charged drop breakup. First the simulations were re-run, with dodecane in the same geometry to define the effects of liquid physical properties on the global evaporation rate. Then the geometry was rescaled to simulate a typical small direct injection engine and a range of injection scenarios were evaluated to obtain an optimum fuel spray dispersal and evaporation performance.

The first step was an examination of the effect of replacing gasoline with a relatively non-volatile hydrocarbon fuel (such as JP-8) in a spark ignition engine. To this end, we started with the computational model defined in Shrimpton and Laoonul [2] and replaced the iso-octane fuel with dodecane, a major constituent of JP-8 and compared the spray development and global evaporation history between these two fuels for the range of spray charge densities and injection timings defined in [2].

Figures 20 and 21 show the time history of various global spray properties, normalized by the maximum, for early and late injection where:

- Black: number of drops present in the domain
- Green: cumulative number of drops hitting the wall
- Blue: liquid drop mass present in the domain
- Cyan: evaporated liquid mass
- Magenta: mean liquid spray specific charge
- Yellow: mean drop diameter

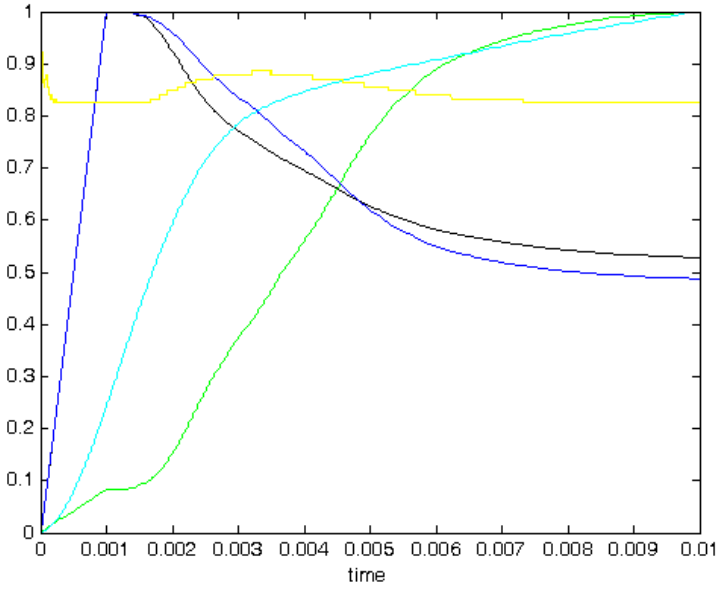

Figure 20: Early injection, no charge.

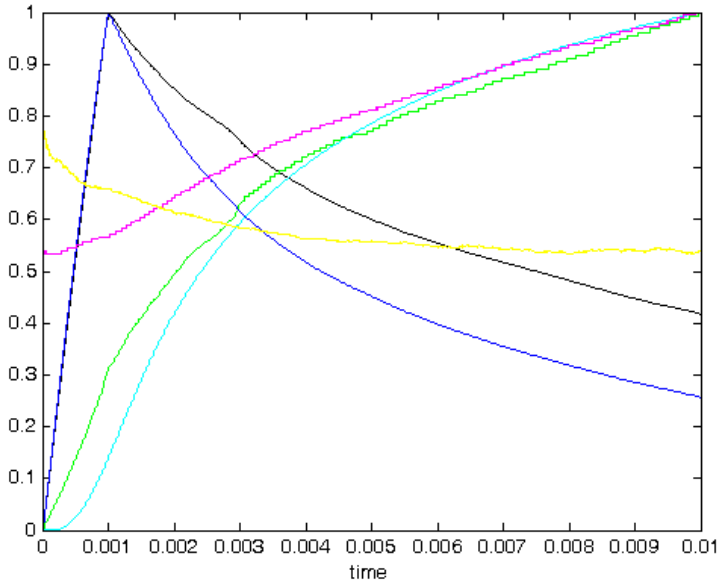

Figure 21: Late injection, 10 C/m^3 specific charge.

It can be seen that virtually no liquid evaporation is occurring during early injection. However, even for late injection, we have 30% of the drop mass still to evaporate. These preliminary results suggested that we do need to reduce the drop diameter generated by the atomizer, even with high levels of mean spray charge.

For the small engine simulations we decided to adopt the Fuji engine purchased and currently being tested at the Army's Vehicle Technology Directorate. This is a single-cylinder, 4-stroke engine with a 39 mm bore and a 28 mm stroke. All other spray and in-cylinder conditions will be taken from [2]. The exception is the fuel mass injected per injection and here we ratioed the fuel mass injected to the downsized engine, by relating the cylinder volume from [2] to that of the Fuji engine. The volume ratio is 0.133, giving a revised injected fuel spray mass injection rate of 1.33×10^{-3} kg/s.

We first conducted a set of simulations for the Fuji engine geometry under an isothermal, non-evaporating assumption with no drop break up model activated. Figure 22 shows the spray generated by a solid cone and a pressure swirl atomizer, with the same mean injection speed, at 0.9 ms after the start of injection. The cylinder conditions reflect injection into the intake stroke, and there pressure and temperature are ambient. In both cases a spray charge of 5 C/m^3 has been applied to the liquid. We can observe that for the solid cone jet a sheath of drops is repelled from the spray centreline; however, a significant fraction remains near the axis, and the penetration rate is worryingly large. The swirl generated atomizer provides excellent spray dispersion and minimal spray penetration, and therefore seems to be the most promising candidate, based on these preliminary results.

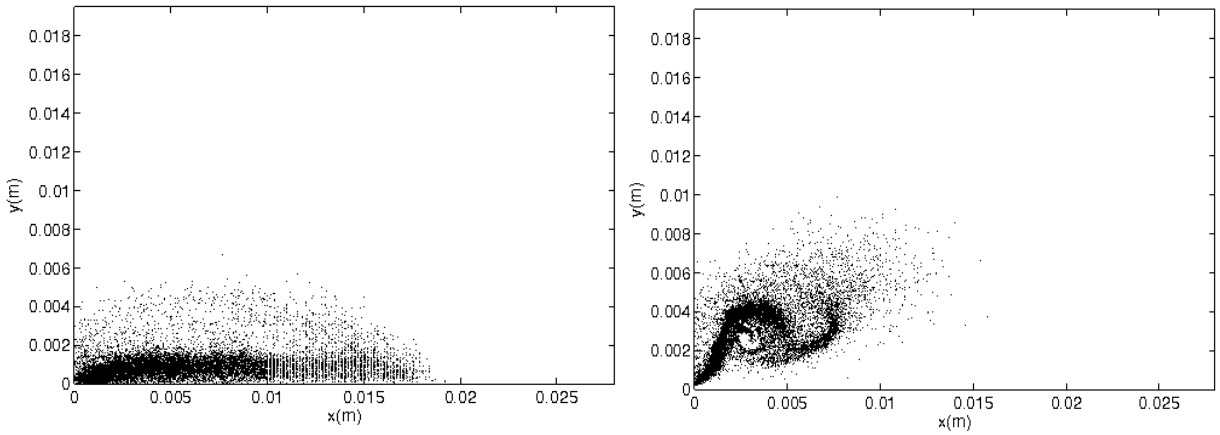

Figure 22: Solid cone (left) and pressure swirl (right) generated sprays injected into ambient air with a spray specific charge of 5 C/m^3, at 0.9 ms after the start of injection – isothermal, non-evaporating conditions.

Next, we conducted simulations for the Fuji engine with a non-isothermal, evaporating assumption with no drop break up model activated. Figure 23 shows the spray generated by a solid cone and a pressure swirl atomizer, with the same mean injection speed, at 0.9 ms after the start of injection. Again, the cylinder conditions reflect injection into the intake stroke, and there pressure and temperature are ambient. In both cases a spray charge of 5 C/m^3 has been applied to the liquid. Comparing these results to those of the isothermal simulation presented in Figure 22, we find a small decrease in the penetration rate for the jet case, by virtue of the small reduction in diameter. However, this effect is marginal at this gas density and pressure.

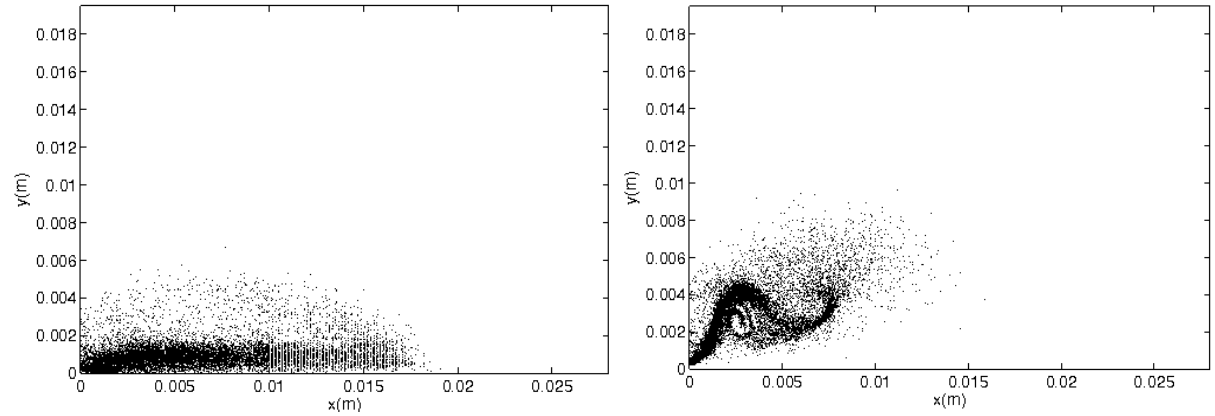

Figure 23: Solid cone (left) and pressure swirl (right) generated sprays injected into ambient air with a spray specific charge of 5 C/m^3, at 0.9 ms after the start of injection – non-isothermal, evaporating conditions.

Finally, we considered the case for a non-isothermal, evaporating assumption with drop breakup models activated under similar conditions as in Figs. 22 and 23. Figure 24 shows the spray generated by a solid cone and a pressure swirl atomizer. Comparing these results to those of the previous simulations presented in Figs. 22 and 23, we find a further small decrease in the penetration rate for the jet case, by virtue of secondary atomization. However, this effect is also marginal at this gas density and pressure.

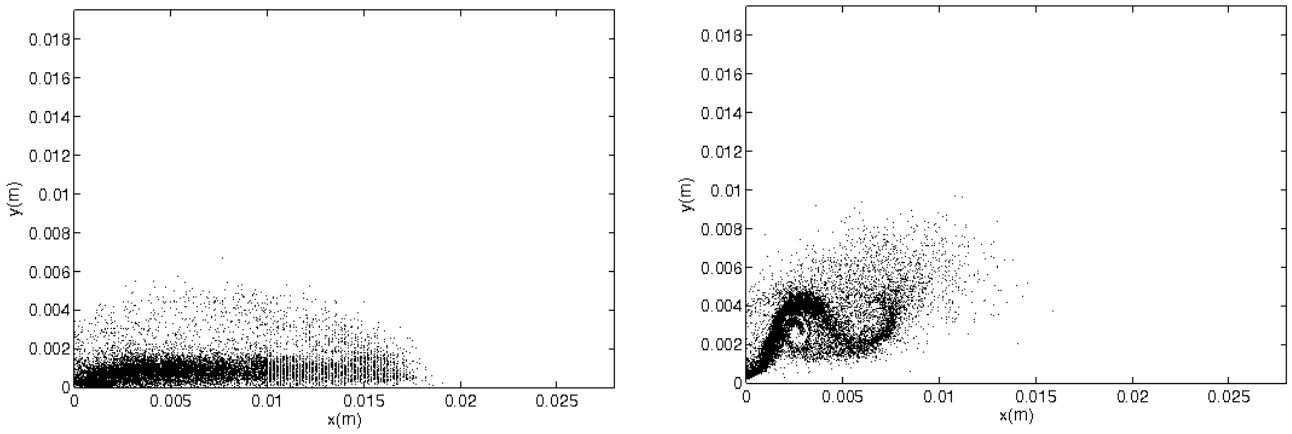

Figure 24: Solid cone (left) and pressure swirl (right) generated sprays injected into ambient air with a spray specific charge of 5 C/m^3, at 0.9 ms after the start of injection – non-isothermal, evaporating condition with droplet secondary breakup.

II.3 Charge injection boundary condition verification in 1D

Description of the transport of free charge starts with considering charge conservation over an arbitrary volume such that $\bar{J}$, the free charge flux is conserved,

$$\frac{d\rho_f}{dt} + \nabla.\bar{J} = S \tag{1}$$

with

$$\bar{J} = \rho_f \bar{u} + \kappa \rho_f \bar{E} + k_D \nabla \rho_f \tag{2}$$

where the rhs of (2) gives, from left to right, contributions from (a) convection of charge by bulk motion of the medium (b) convection of charge by the electric field and (c) diffusion of charge through the medium respectively. In (2), κ and k_D are the charge carrier mobility and diffusion coefficients for the particular combination of charge carrier and medium. For ideal gases and liquids k_D and κ are linked via the Einstein relation,

$$k_D = (kT\kappa)/q \tag{3}$$

where k is the Boltzmann constant, T the absolute temperature and q the individual particle charge. An approximate relation, valid for negative ions in highly insulating liquids, between κ and μ_l has the form,

$$\kappa = 3 \times 10^{-11} / \mu_l \tag{4}$$

Equation (1) and the Poisson equation will be discretized using the finite volume technique and a suitable analytical test problem devised to confirm the linkage between the transport of space charge and the electric field which are tightly coupled. The problem here is amplified by the fact that the

source term expressions are non-linear thus the test case used here for ρ_f is defined by the electrical source term alone. Space charge is injected at a constant rate of 1 mA at x=L between two flat conducting metal plates positioned at x=0 and x=2L. Thus the boundary conditions that define the analytical model are $\phi_{x=0=2L}=0$, $E_{x=L}=0$ and $J_{L>x>0}=-J_{2L>x>L}$=constant and allow a simulataneous one-dimensional solution for rectangular geometry which gives,

$$\phi^* = \frac{3\phi}{2L}\left(\frac{2J_0L}{\kappa\varepsilon_f\varepsilon_0}\right)^{-1/2} = \left(\frac{x}{L}-1\right)^{3/2} - 1,$$

$$E^* = E\left(\frac{2J_0L}{\kappa\varepsilon_f\varepsilon_0}\right)^{-1/2} = \left(\frac{x}{L}-1\right)^{1/2}, \rho_f^* = \rho_f\left(\frac{J_0\varepsilon_f\varepsilon_0}{2\kappa L}\right)^{-1/2} = \left(\frac{x}{L}-1\right)^{-1/2}$$

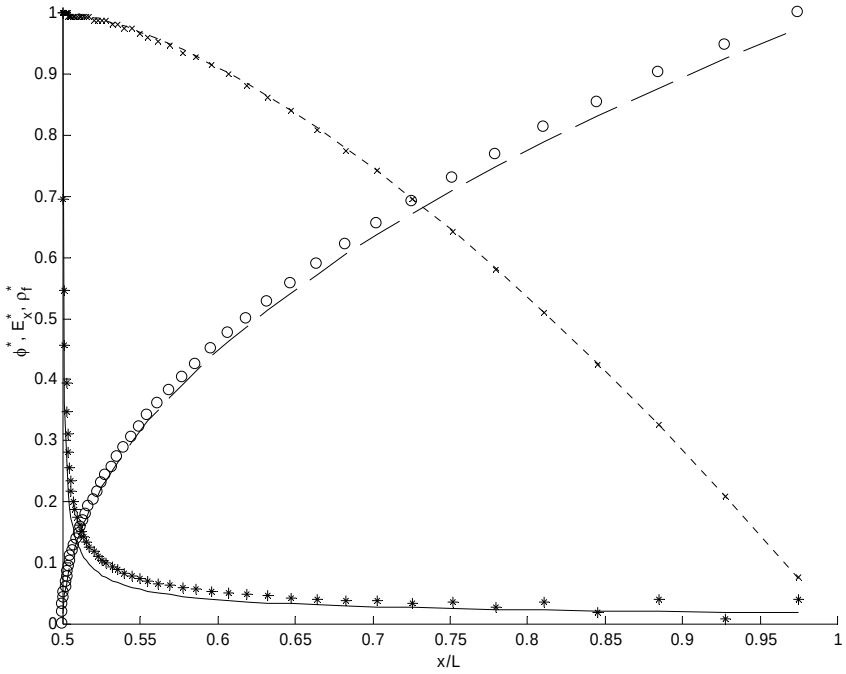

Figure 25: Analytical (lines) and numerical (symbols) to the space charge injection problem.
x: ϕ **;** $\bigcirc$**:** E **;** ***:** ρ **.**

The numerical solution of this problem is given in Figure 25. The primary features of the analytical solution and reasonable accuracy is obtained, though the accurate resolution of the extreme gradient of space charge in the injection zone is a formidable numerical challenge and will require some approximation in the full EHD simulation in the nozzle flow simulation.

II.4 Nozzle internal flow simulation

This part of the study aims to simulate the coupled EHD fluid mechanics within the atomizer, between the high voltage electrode and the nozzle orifice. The near orifice region of Fig. A.2 in Appendix A has been defined using a finite volume 2D mesh, as shown in Figure 26. Here the y=0 line represents the axis and the $x = x_{\max}$ plane the external face of the atomizer. The flow channel is meshed, the south-

west wall section the high voltage electrode and the north-east section the earthed nozzle body. Realistic dimensions have been taken from earlier experimental work detailed in Part I of this report.

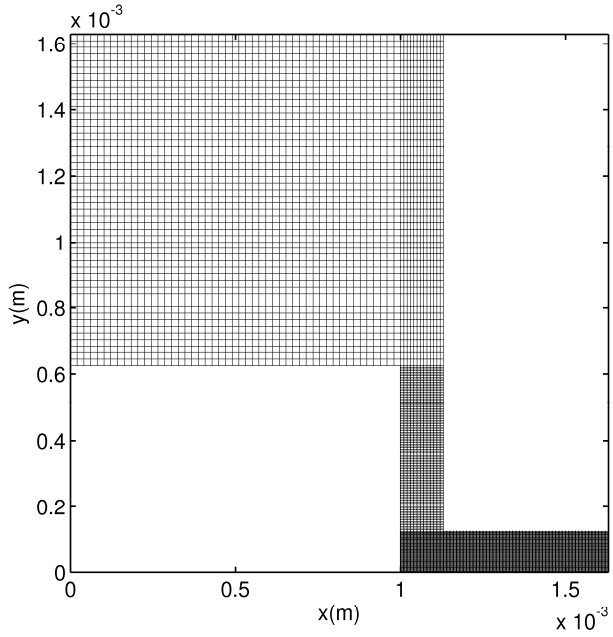

Figure 26: Computational domain for the EHD flow.

First, we report basic non-coupled electrical and flow results to confirm that the model is well posed and the computational code is operating correctly and sensibly.

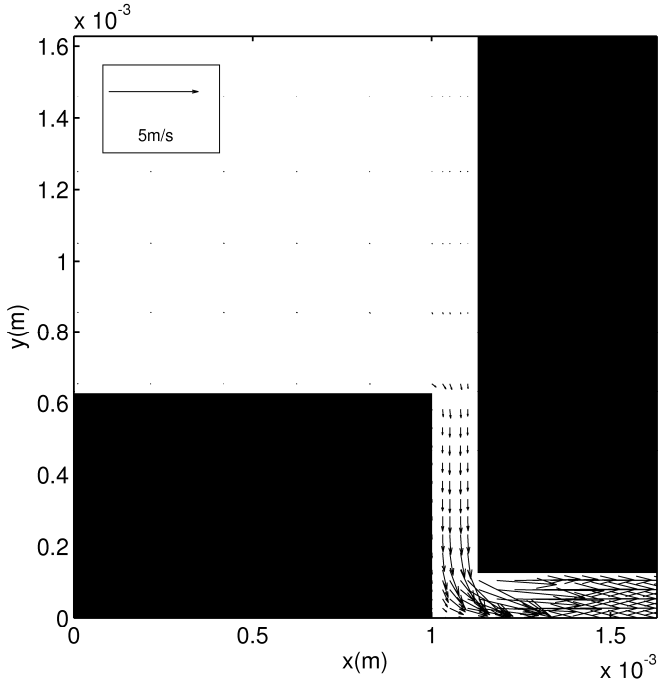

Figure 27: Velocity vectors.

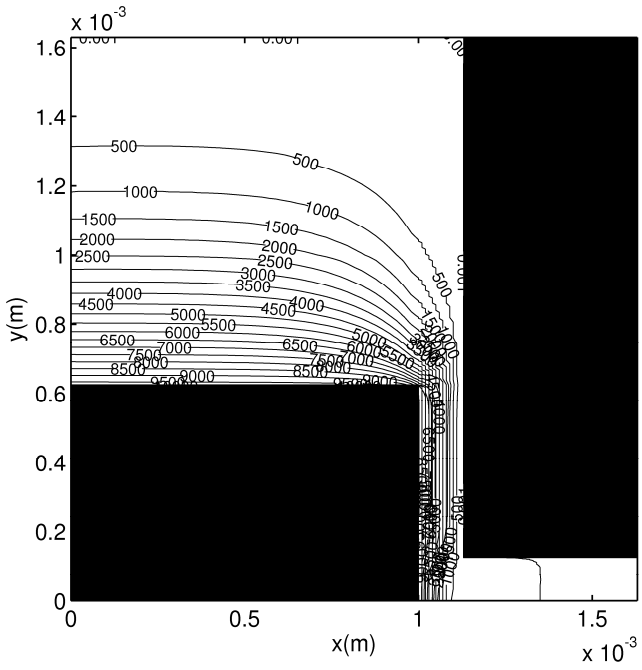

Figure 28: Voltage contours.

Figures 27 and 28 show the velocity field with an imposed mean injection velocity, based on the orifice channel, of 10 m/s and the voltage field, where 10 kV is imposed on the high voltage electrode. Figure 28 reveals the likely location of the charge injection, near the corner of the high voltage electrode where the field magnitude is greatest. These preliminary results confirm correct set-up and prediction of the domain.

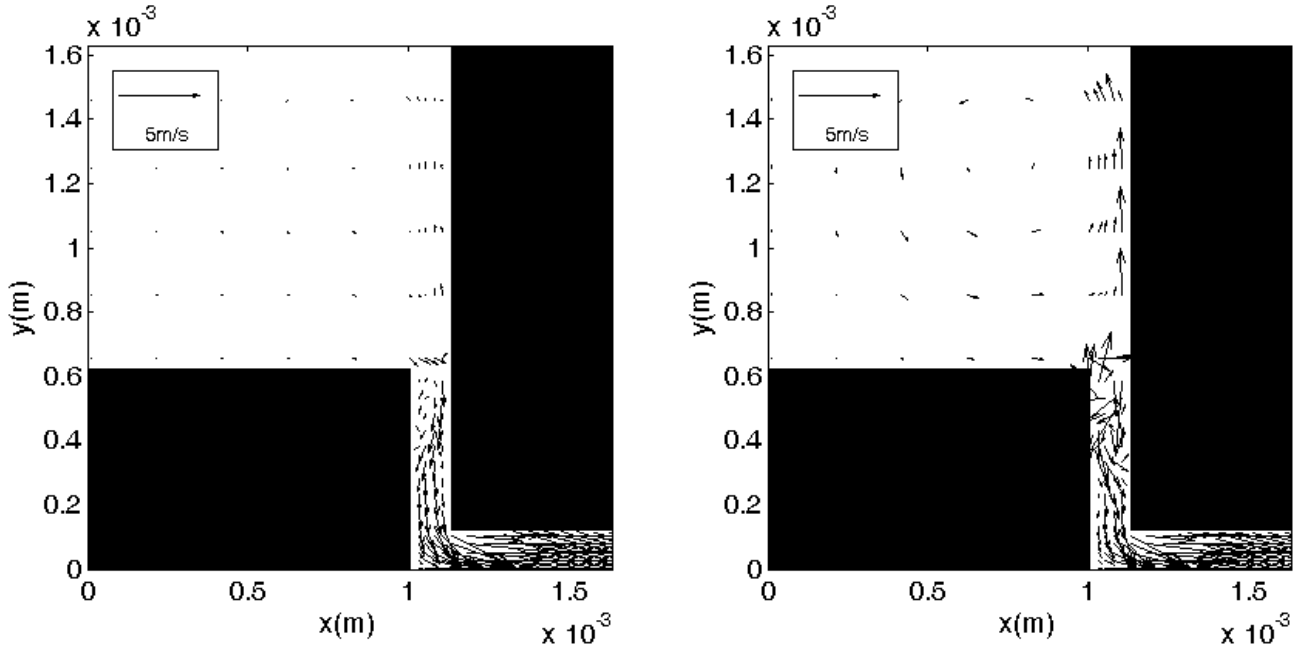

Figure 29: Coupled EHD flow for current injected from 4 kV (left) and 9 kV (right) electrodes.

Next we show the coupled EHD, where it is assumed that the charge is injected into the domain at the corner of the high voltage electrode, i.e. $(x, y) = (1.0, 0.6)$. The voltage-current relationship used is taken directly from experimental data obtained earlier in this project.

Figure 29 should be compared to Fig. 28, and it should also be noted that the velocity vector scaling is identical between these figures. The 4 kV result shows two vortex structures, one small and between the high voltage and earthed electrode, downstream of the charge injection point. There is also a larger vortex rotating in the opposite direction. As the voltage (and current) increased (Fig. 29, right) these flow features are amplified and the flow becomes rather chaotic. These results seem to confirm other research in the literature that suggests different injection regimes leading to differing flow instability regimes.

PART III: Development of engine test system and port injection system

The following is a quick overview of the planning of our Small Engine Laboratory. Listed are the components that will be contained in the lab. The first component acquired is a Fuji-Imvac 4-stroke engine (Fig. 30), a duplicate of the engine currently under test at VTD.

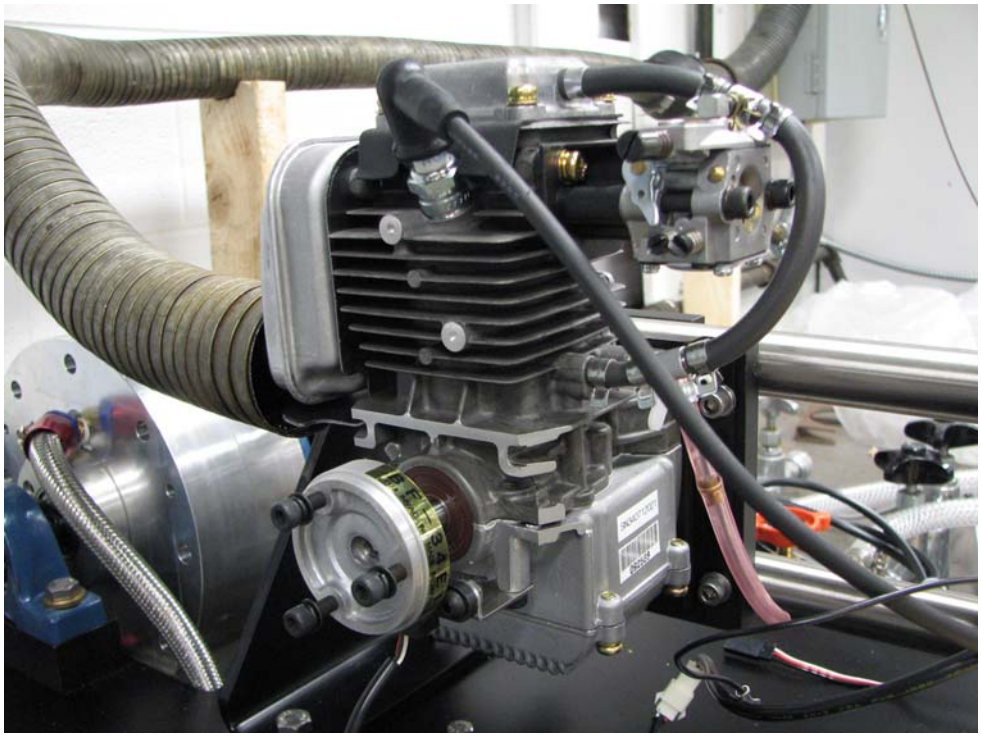

Figure 30: Fuji –Imvac 4-stroke engine.

The engine carries a displacement of 34 cubic centimeters and produces about 1.6 horsepower at 7,500 revolutions per minute. From the factory the engine runs with gasoline using a carburetion system. The next component obtained is a dynamometer from Trik-Dyno, LLC.

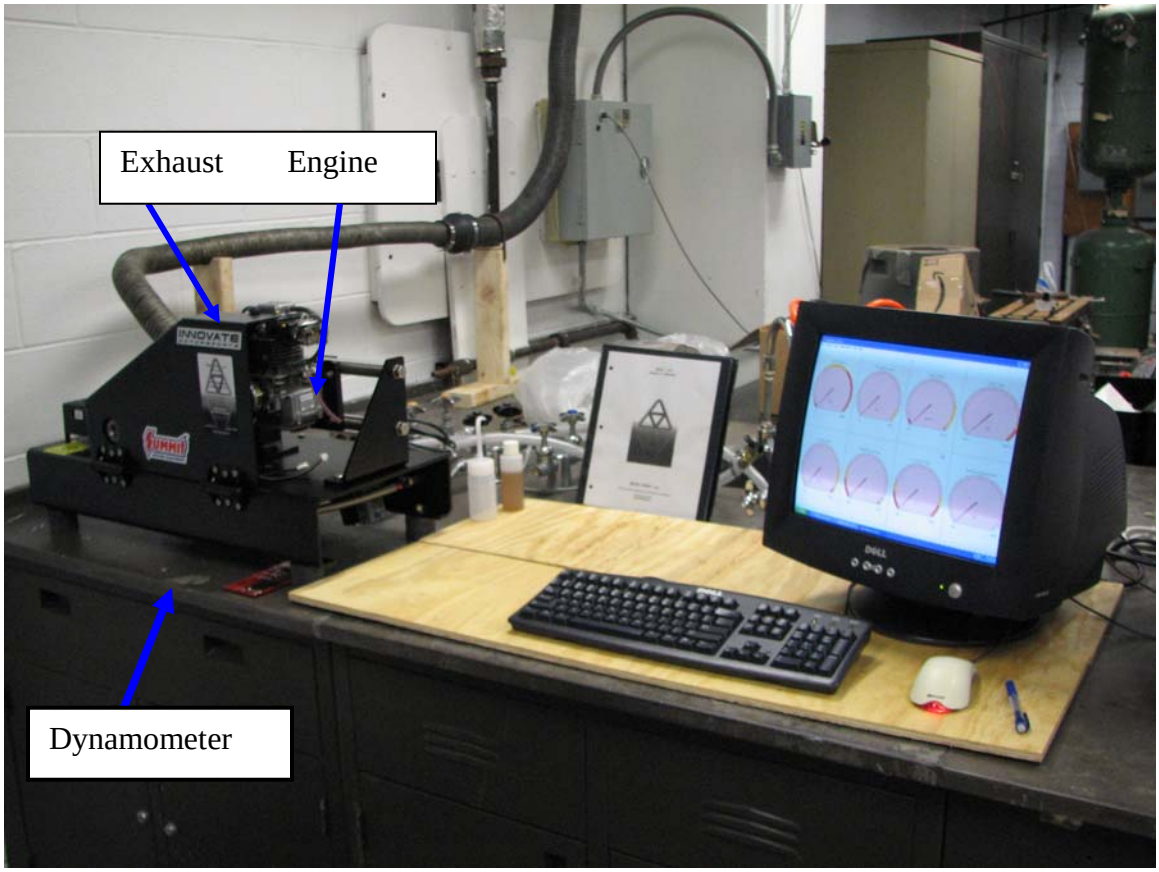

Figure 31: Dyno setup.

This will allow us to measure power output and performance of the Fuji-Imvac engine under various conditions. Data acquisition and monitoring software are to be used in conjunction with the engine and dynamometer as can be seen in Fig. 31.

The next component that will act as an observational learning tool is a fuel injection demonstration setup. It consists of a fuel tank, a fuel pump, fuel rails and injectors controlled by a stand alone electronic fuel management system manufactured by Megasquirt (Fig. 32).

A signal will be generated using Labview and sent to the computer system to pulse the injectors. This will be useful in learning how fuel injection works and how to control the operational characteristics of a fuel injection system.

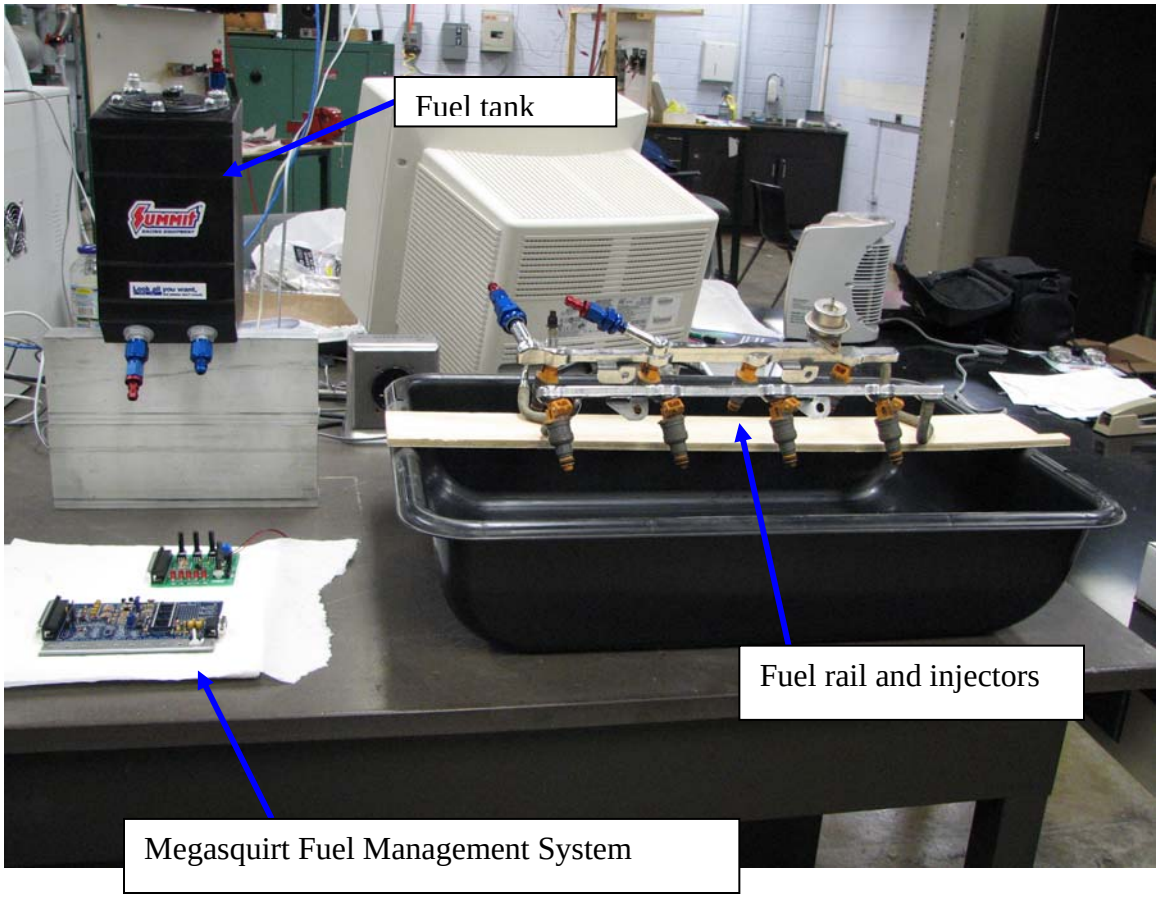

Figure 32: Programmable fuel injection system.

PART IV: Summary of capabilities developed for Phase II

NOTE: Enabling Energy Systems Inc. has received a matching fund for $99,999 from the State of Indiana for this Phase I STTR project. This additional fund will allow the company to continue its work on this project beyond the expiration of Phase I through mid 2009 when Phase II awards will be selected. The State of Indiana also provides matching fund for Phase II awards.

Below, we provide a summary of our capabilities developed based on Phase I activity and partial utilization of the Indiana matching fund:

Charge injection: atomizer experiments

- **Proved that low-conductivity JP-8 works very well with charge injection technology** – we can use our extensive empirical database to guide atomizer development.
- Adapted an existing charge injection atomizer to accommodate multiple orifice designs which permit small mean drop diameter at low pressure drops.

Engine technology and measurement systems

- Conducted a timescale study that allows us to predict target drop diameter required for a small engine running on JP-8. Good estimates of the improvement of global evaporation rate possible by adding electric charge.
- Liased with the army research lab and installed a duplicate of their test bed and engine to coordinate research testing and development for Phase II.
- Development and extension to off-the-shelf port fuel injection systems for retro-fitting to the small engine – will provide a fuel economy and emissions improvement over the existing carburetor and gives a step towards fitting an EHD injector.
- Development of optical measurement systems to accurately characterize the spray – further guide the spray development.

Pulsed charge injection

- Developing two technology options – a pulsed EHD atomizer and a segmented system where the charge injection device operates in steady state and uses standard atomizer units – enables us to provide a range of options based on cost, complexity and provides many opportunities beyond Phase II.
- Development and evaluation of multiplexed blade based charge injection systems – permit arbitrarily large injection currents in a very simple and robust device.

Spray modeling

- Adapted an existing validated CFD code for small engines and JP-8. Allows us to probe and evaluate cheaply and effectively choice of atomizer spray type, injection timing, amount of charge to use to minimize wall wetting whilst maximizing homogeneity of the fuel vapor/air mixture – permits detailed optimization studies to be performed.

Internal flow modeling

- Proven a method to define the charge injection boundary condition at the high voltage electrode.
- Acquired a good understanding of the nature of the physics present – level of EHD generated chaos – permits better solution strategies to be developed.
- Applied a method to numerically solve the coupled EHD system and to provide example results of a simple EHD atomizer internal flow – this will enable us to understand the EHD coupling present in the complex pulsed injection system.

References

[1] Edwards, T. and Maurice L. Q., "Surrogate mixtures to represent complex aviation and rocket fuels," *Journal of Propulsion and Power*, **17**(2), pp. 461-466, 2001.

[2] Shrimpton, J. S. and Laoonual, Y., "Dynamics of electrically-charged transient evaporating sprays," *International Journal for Numerical Methods in Engineering*, **67**(8), pp. 1063-1081, 2006.

Appendix A: Multi-orifice charge injector – design details

The previously used point-plane atomizer was modified as follows:

The needle electrode was replaced with 3.18 mm diameter blunt Tungsten electrode. Parts from the point to plane atomizer which were modified to accommodate the new blunt Tungsten electrode bar are: PTFE_TOP_INSULATOR, HV_ELECTRODE_COUPLING, PTFE_INSULATOR and NOZZLE (see Fig. A.1). Three different Tungsten electrodes with blunt tip shapes were used. These are "flat sharp edge," "flat round edge" and "round tip" shapes.

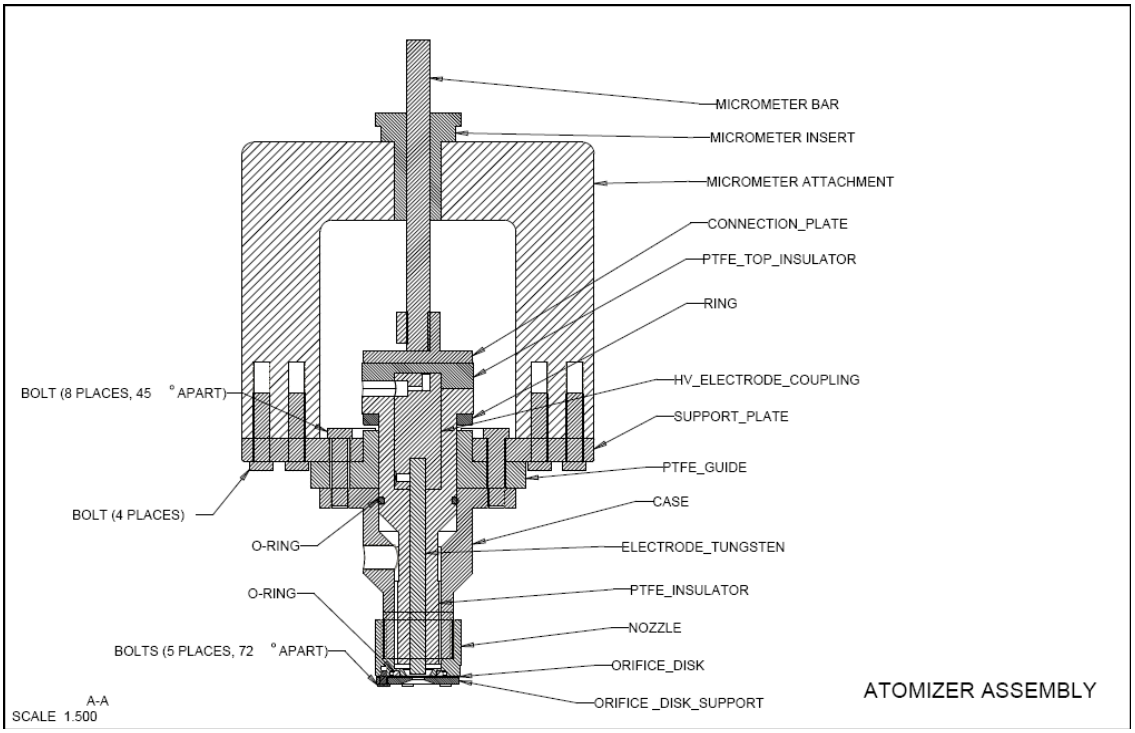

Figure A.1: Schematic of the blunt electrode atomizer assembly.

The Nozzle was modified in order to attach a separate orifice disk to it. Separate orifice disks were used to allow drilling different orifices sizes and patterns without the need to change nozzle. Orifice disk is bolted and sealed against nozzle bottom flat surface and supported by ORIFICE_DISK_PLATE made from stainless steel to prevent orifice disk deflection under applied fluid pressure (Fig. A.2). Orifice disks are made from 0.50 mm thickness brass disks.

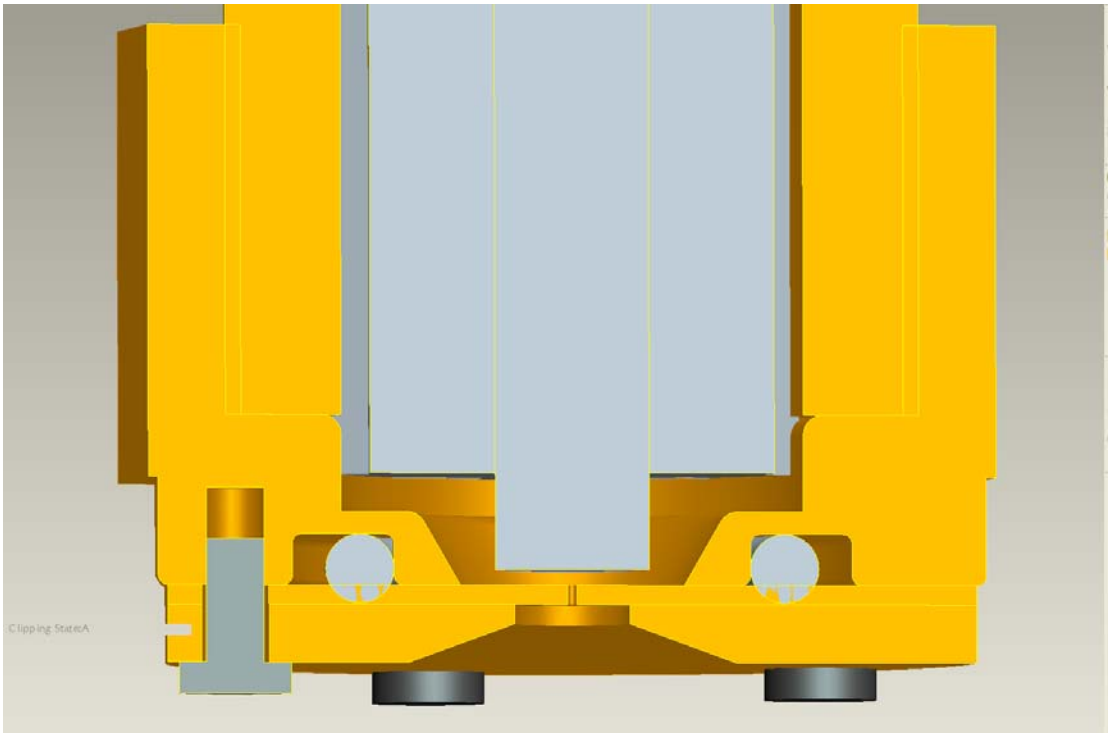

Figure A.2: Atomizer assembly 3D half section CAD assembly shows the details of orifice inlet and orifice disk attachment to nozzle.

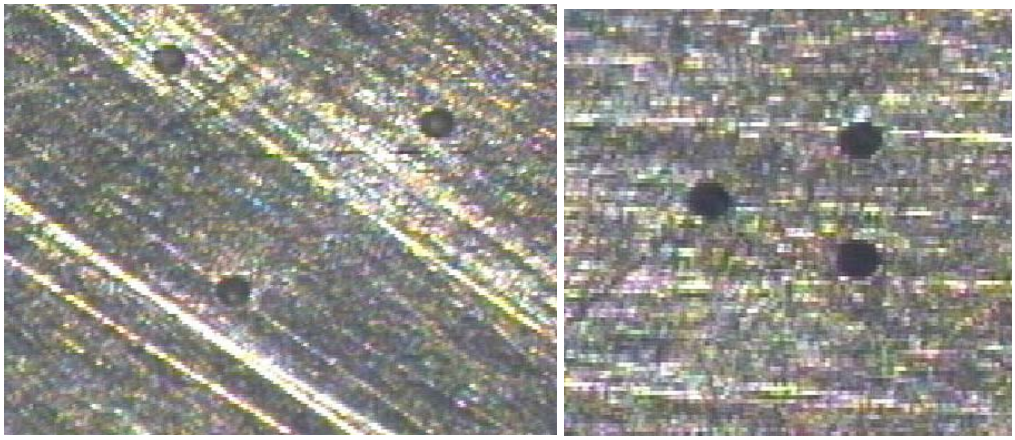

Figure A.3: A 3 x 125 micron orifice array drilled on a 1 mm and a 0.5 mm pitch.

Figure A.3 shows a 3 x 125 micron orifice array drilled on a 1 mm and a 0.5 mm pitch. These were evaluated to examine the possible detrimental effect of the proximity of one jet to another.

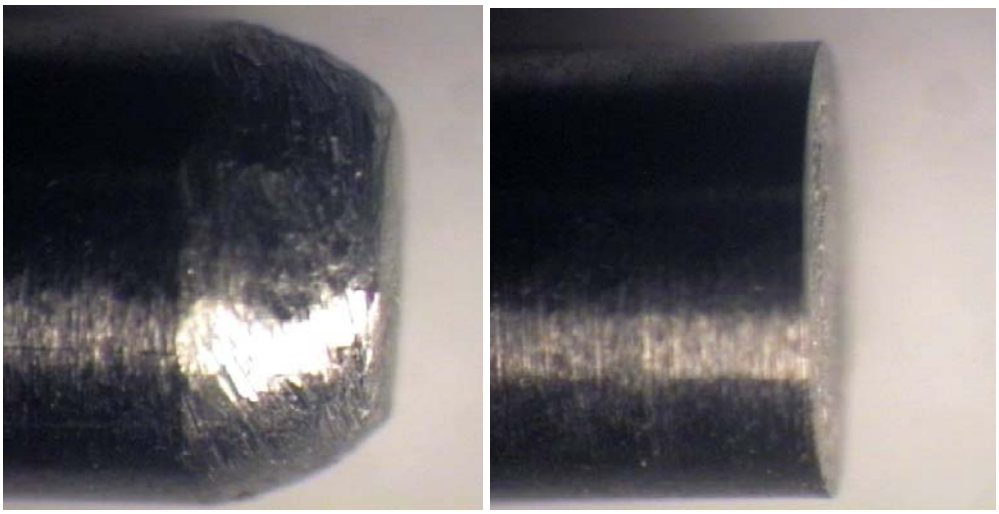

Figure A.4: Two variations of emitter surface shape of the 3 mm tungsten bar.

Figure A.4 shows two variations of emitter surface shape of the 3 mm tungsten bar tested in the modified atomizer. Note that to mitigate the increased radius of curvature in the tip on the left the surface has been artificially roughened.